Single-molecule observation of protein adsorption onto an inorganic surface

Supporting Information

David J. Niedzwiecki,[1] John Grazul,[2] and Liviu Movileanu[1,3,4]

[1]*Department of Physics, Syracuse University, 201 Physics Building, Syracuse, New York 13244-1130, USA*

[2]*Cornell Center for Materials Research, 627 Clark Hall of Science, Cornell University, Ithaca, New York 14853, USA*

[3]*Structural Biology, Biochemistry, and Biophysics Program, Syracuse University, 111 College Place, Syracuse, New York 13244-4100, USA*

[4]*Syracuse Biomaterials Institute, Syracuse University, 121 Link Hall, Syracuse, NY 13244, USA*

Key words: Single-molecule Biophysics; Nanobiotechnology; Low-stress Silicon Nitride; Bovine Serum Albumin; Solid-state Nanopore; Liquid-solid Interface

Correspondence/reprint requests:
Liviu Movileanu, PhD, Department of Physics, Syracuse University, 201 Physics Building, Syracuse, New York 13244-1130, USA; Phone: 315-443-8078; Fax: 315-443-9103;
E-mail: lmovilea@physics.syr.edu

1. Nanopore fabrication

Solid-state nanopores were manufactured by electron beam drilling of a 20 nm-thin free-standing layer of Si_xN_y. The Si_xN_y layer was supported by a silicon frame. The substrate was fabricated by standard photolithography techniques (**Fig. S1**) at the Cornell NanoScale Science & Technology Facility (CNF). Si_xN_y was deposited onto a silicon wafer by low-pressure chemical vapor deposition (LPCVD). Nitride was removed from one side of the wafer and contact lithography was used to pattern a square that was back-etched with KOH to form a free standing window of Si_xN_y. This method has been described elsewhere.[1] Nanopores were drilled using a FEI Technia F-20 Scanning/Transmission Electron Microscope (S/TEM) at the Cornell Center for Materials Research (CCMR). To drill the nanopores, a high intensity electron beam was focused on the surface of the nitride substrate. Drilling was performed in the scope's STEM mode using a spot size of 1 nm. The accelerating voltage of the STEM was 200 kV and the beam current was 0.03 nA. Using a 20 nm-thin membrane of Si_xN_y, nanopores with a diameter of ~7 nm formed within ~1 minute (**Figs. S2-S3**). For wide nanopores, in the range of 8-20 nm, the diameter was increased by longer exposure or movement of the spot along the edges of the nanopore. Nanopores with a diameter less than 7 nm were formed by pore shrinking.[2] After the initial nanopore was formed, shrinking was achieved by reducing the beam intensity of the STEM. This causes the nitride around the nanopore to "fluidize" and shrink in a highly controlled manner. Using this approach, nanopores, as narrow as 2 nm, can be fabricated in Si_xN_y films. The solid-state nanopores were imaged in the TEM mode to determine their inner diameter (**Fig. 1**).[2]

2. Single-channel current recordings with solid-state nanopores in ultra-thin Si_xN_y membranes

In these experiments, single-channel current measurements[3,4] were carried out using an Axon 200B patch-clamp amplifier (Axon, Foster City, CA) in the voltage-clamp mode, which was connected to the chamber baths by Ag/AgCl electrodes. The output from this amplifier was also filtered by an 8-pole low-pass Bessel filter (Model 900, Frequency Devices, Haverhill, MA) at a frequency of 10 kHz and sampled at 50 kHz, unless otherwise stated. An Optiplex Desktop Computer (Dell, Austin, TX) equipped with a Digitdata 1440 A/D converter (Axon) was used for data acquisition. Acquisition of data was made using Clampex 10.2 software (Axon) and the analysis was performed using pClamp 10.2 software (Axon). The BSA protein (purity greater than 99%, Bio-Rad, Hercules, CA), used without further treatment in deionized water, was added to the *cis* side of the chamber at low nanomolar concentrations (**Fig. S4**). The *cis* side of the chamber was grounded and a positive current (upward deflection) represents a positive charge moving from the *trans* to *cis* side. All measurements were performed in symmetrical solutions containing 1M KCl, 10 mM potassium phosphate, pH 7.4.

3. Preparation of the silicon nitride membranes

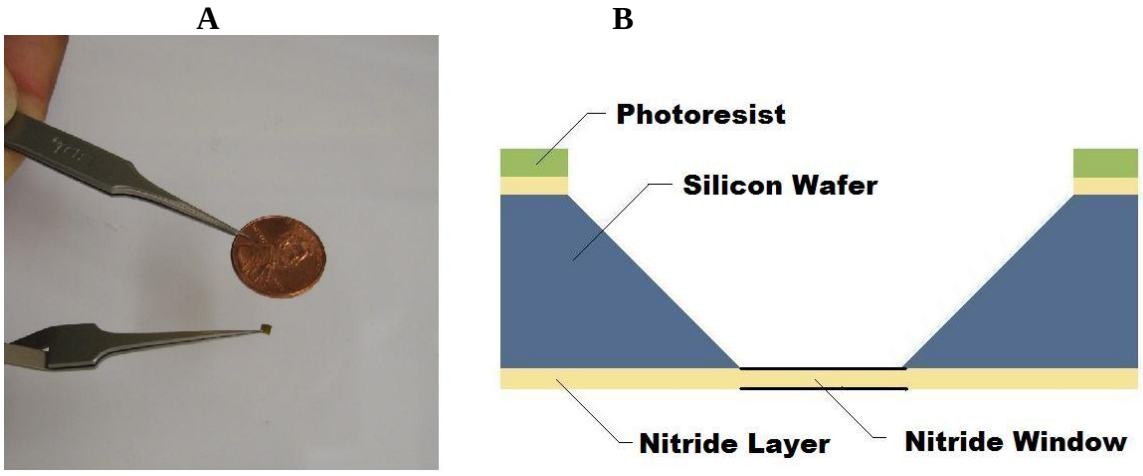

Figure S1. A free standing silicon nitride film of 20 nm thickness was supported by a silicon substrate. Nitride was deposited via a LPCVD furnace. Contact lithography was used to pattern the design of a square window. Plasma etching was used to remove the nitride layer. KOH was employed to etch the silicon and expose the nitride layer. A) The chip, measuring 2.5-by-2.5 mm, is pictured next to a penny for scale. B) A cartoon illustration of the chip in profile. The nitride window measures 50-by-50 μm.

4. Protocols for nanopore treatment

After drilling, the nanopore was placed in a Teflon chamber that consisted of two baths separated by a partition. This partition had a through-hole onto which the nanopore chip was mounted. Thus, the nanopore was the only path through which ions from one bath could move to the other. In order for measurements to be performed, the nanopore had to be "wetted" so that ionic solution entered its interior and formed a connecting bridge between the two baths of the chamber. To insure that solution was in the nanopore, the following protocol was used. Each nanopore was washed for over 20 minutes in boiling Piranha solution (1:4 Hydrogen Peroxide: Sulfuric Acid; Fischer, Sair Lawn, NJ). Treatment with Piranha solution is expected to deposit –OH groups onto the nitride surface, making it hydrophilic.[5,6] Nanopores were then rinsed with degassed, distilled water. After rinsing, the nanopores were dried under suction and immediately sealed into the chamber with Kwik-Cast® (World Precision Instruments, Sarasota, FL). The Kwik-Cast was allowed 10 minutes to cure, after which the chamber was filled immediately with 1 M KCl. To confirm wetting, a current vs. voltage (I/V) curve was constructed. The voltage ramp was raised at a constant rate from -200 mV to 200 mV over a period of 2 minutes and a current response was recorded. A plot of current versus applied potential was made for the I/V curve (see below).

5. Characterization of the nanopores

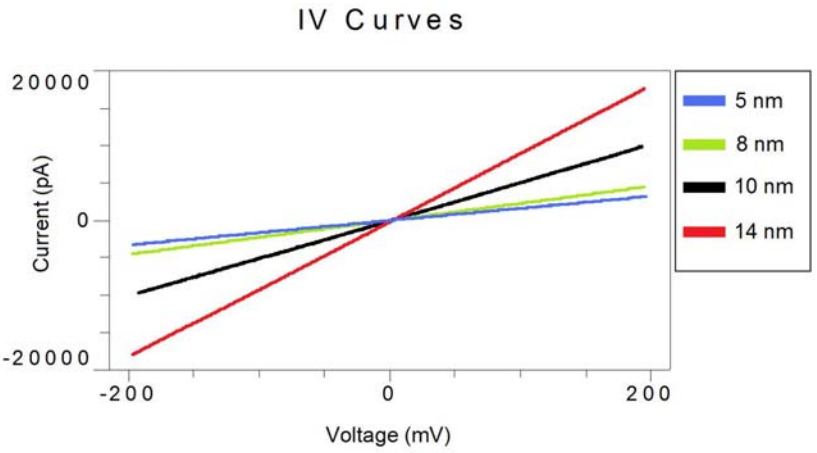

Figure S2. Voltage dependence of the single-channel currents for nanopores of different diameters. Current response measurements were taken at 1 M KCl, 10mM potassium phosphate buffer, pH 7.4.

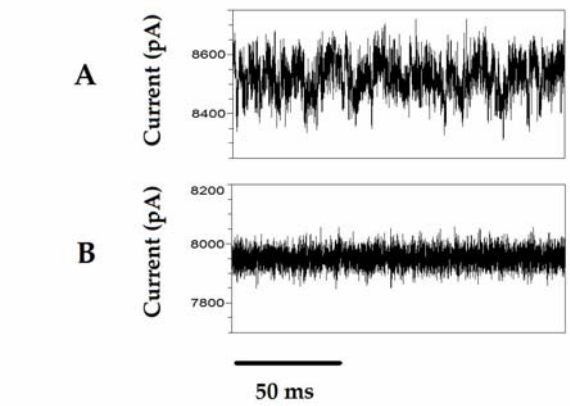

Figure S3. Comparison traces of nanopores. A) A trace collected with a 10 nm-diameter nanopore with a "noisy" current signature, B) A trace collected with a 10 nm-diameter nanopore with a stable single-channel current. Measurements were taken at a transmembrane poteantial of +150 mV, with a buffer solution containing 1M KCl, 10 mM potassium phosphate solution, pH 7.4. The single-channel electrical traces were low-pass Bessel filtered at 10 kHz.

A nanopore was considered to be "wet" if the following three properties were observed. First, the nanopore had to show a stable conductance at a constant applied transmembrane potential. Transmembrane potentials of +150 mV were typically used for this test (**Fig. S3**). Second, the current response had to be linear (Ohmic) with the applied transmembrane potential (**Fig. S2**). Third, the conductance, as measured by a straight-line, least-squares fitting of the I/V curve, had to correspond with the expected value of the conductance for a nanopore of the diameter measured via TEM. Expected conductance values were obtained in the following way. The nanopore diameter was measured with TEM. Conductance of nanopores satisfying the first two criteria was characterized at 1M KCl using the I/V curve protocol described above. The results were comparable to those found in the liturature.[7] For our purposes, if the nanopore conductance was within 20% of the expected value, the nanopore was considered acceptable.

6. BSA Purity

Lyophilized bovine serum albumin (BSA)[8] was purchased from Bio-Rad (Hercules, CA). BSA was hydrated with double-distilled water to a concentration of 22 µM and stored at 4°C. Purity

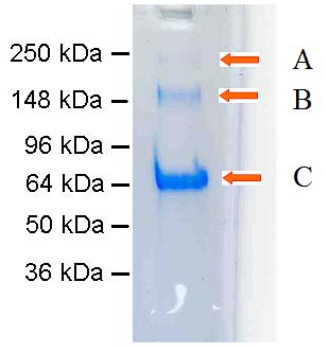

was confirmed by 10% SDS-PAGE gel electrophoresis (**Fig. S4**). Bands consistent with BSA monomers, dimmers and trimers were observed.

Figure S4. SDS-PAGE gel electrophoresis of the BSA sample. (A) BSA trimers, (B) BSA dimmers (C) BSA monomers. BSA-SDS was heated to 95°C for 5 minutes prior to running the gel.

7. The amplitude of the short--lived current blockades

Figure S5

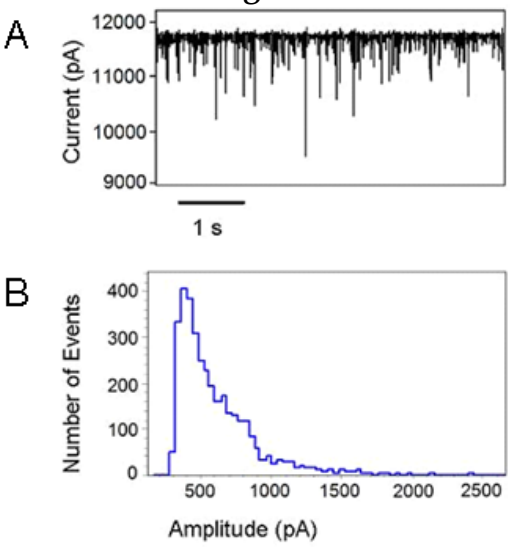

Figure S5. Typical single-channel current trace (A) and typical event amplitude histogram (B) recorded with a 12 nm-wide solid-state nanopore when 60 nM BSA was added to the *cis* chamber. The buffer solution contained 1 M KCl, 10 mM potassium phosphate, pH 7.4. The applied transmembrane potential was +150 mV. The single-channel electrical traces were low-pass Bessel filtered at 10 kHz.

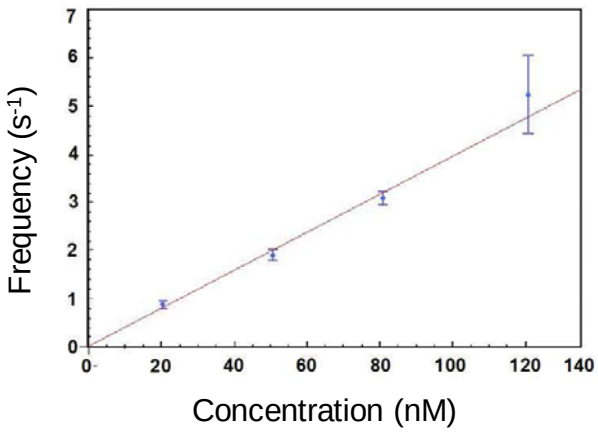

Figure S6. Dependence of the short-lived event frequency on the BSA concentration added to the *cis* chamber. The single-channel electrical data were recorded with a 12 nm-diameter nanopore. Least squares fitting gave a slope of 26 $s^{-1}nM^{-1}$ BSA. Other experimental conditions were similar to those presented in **Fig. S5**.

Our estimate for the frequency of the short-lived current blockades did not include the missed events due to the rise time of the Bessel filter.[9] The frequency of the short-lived current blockades was calculated by dividing the number of current blockades by the duration of the trace. Assuming that the current blockades occurred stochastically, uncertainty values for frequency were calculated from the uncertainty in the number of current blockades given by

$N^{1/2}$, where N is the number of current blockades.[10] This value for uncertainty assumes that the short-lived current blockades occurred independently and continuously following a Poisson process. Nanopores varied in sensitivity to BSA. Different nanopores of the same diameter showed up to a 60-fold difference in the frequency of events under the same conditions. For example, we observed that the frequency of current blockades with two 12 nm-diameter nanopores (at +150 mV; 1M KCl, 10 mM potassium phosphate, pH 7.4; 180 nM BSA) was 0.5 ± 0.03 s^{-1} and 37.5 ± 0.25 s^{-1}, respectively. The median amplitude of the short-lived current blockades was independent of the diameter of the nanopore (470 ±40 pA, for 19 nanopore diameters ranging 9-20 nm) (**Table S1**). This is to be expected, if these current blockades feature amplitude that is proportional to the excluded volume of the BSA proteins.

Table S1

Diameter (nm)	Median amplitude of blockades (pA)
9	524
10	488
10	554
12	441
12	448
12	449
12	457
12	528
12	464
12	462
16	430
16	422
16	438
16	428
20	453
20	515
20	496
20	516
20	421

Table S1. Median amplitude values for nanopores of given diameter were found by performing a single-channel search with Axon ClampFit 10.2 analysis package. All measurements were performed at 1M KCl, 10 mM potassium phosphate, pH 7.4, with an applied voltage of +150 mV.

This proportionality, as seen in the relation $\Lambda \cong \frac{H_{eff}^{2}\,\Delta I_b}{\sigma V}$, can be arrived at by considering the change in conductivity induced by a non-conducting spherical obstruction of diameter d_p in a cylindrical pore with diameter d_m and effective length H_{eff}. Following DeBlois and Bean,[11,12] we make the approximation that the resistance of the nanopore may be expressed as, $R = \int \frac{dx}{\sigma A(x)}$, where $A(x)$ is the cross sectional area perpendicular to the length coordinate x and σ is the conductivity of the solution. Assuming $\{d_p > 0, d_m > 0, d_p > d_m\}$, the resistance of the nanopore with the obstruction may be expressed as

$$R_b \to \int_0^{H_{eff}-d_m} \frac{1}{\pi\left(d_p/2\right)^2\sigma}dx + \int_0^{d_m} \frac{1}{\left(\left(d_p/2\right)^2 - \left(\left(d_m/2\right)^2 - \left(\left(d_m/2\right)-x\right)^2\right)\right)\pi\sigma}dx .$$

$$R_b = \frac{4}{\pi\sigma}\left(\frac{H_{eff}-d_m}{d_p^2} + \frac{ArcTan\left[\frac{d_m}{\sqrt{-d_m^2+d_p^2}}\right]}{\sqrt{-d_m^2+d_p^2}}\right).$$

Then, the nanopore current with the obstruction is given by the following expression,

$$I_b = \frac{V}{R_b} = V \Big/ \left(\frac{4\left(H_{eff}-d_m\right)}{\pi\sigma d_p^2} + \frac{4\,ArcTan\left[\frac{d_m}{\sqrt{-d_m^2+d_p^2}}\right]}{\pi\sigma\sqrt{-d_m^2+d_p^2}}\right),$$

where V is the applied transmembrane potential across the nanopore. The expected change in current is $\Delta I_b = I_0 - I_b$. With the open current of the nanopore $I_0 = \frac{\pi\sigma V d_p^2}{4H_{eff}}$

$$\Delta I_b = \frac{\pi\sigma V d_p^2}{4H_{eff}} - V \Bigg/ \left(\frac{4\left(H_{eff} - d_m\right)}{\pi\sigma d_p^2} + \frac{4ArcTan\left[\frac{d_m}{\sqrt{-d_m^2 + d_p^2}}\right]}{\pi\sigma\sqrt{-d_m^2 + d_p^2}} \right).$$

Expanding in series and retaining up to the cubic term gives:

$$\Delta I_b \cong \frac{\pi\sigma V d_m^3}{6H_{eff}^2}.$$

Using $\Lambda = \frac{4}{3}\pi\left(\frac{d_m}{2}\right)^3$ as the protein excluded volume, we have the following approximate expression:

$$\Lambda \cong \frac{H_{eff}^2 \Delta I_b}{\sigma V}.$$

8. The characteristics of the long-lived current blockades

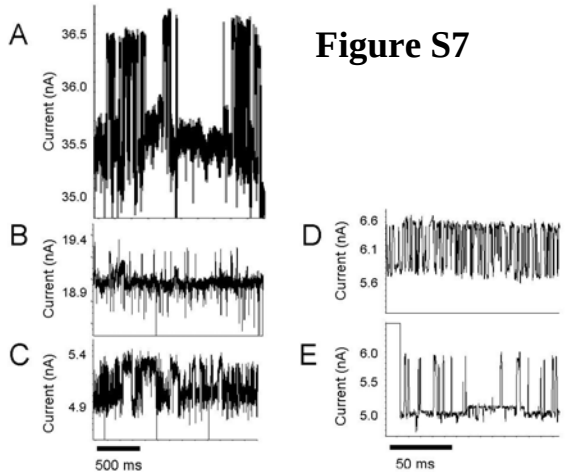

Figure S7

Figure S7. Examples of two-state gating in Si_xN_y nanopores. For all traces, the experimental conditions were 1 M KCl, 450 nM BSA, 10 mM potassium phosphate, pH 7.4. The applied potential was +150 mV. The single-channel traces were low-pass Bessel filtered at 2 kHz. Nanopores A, B, C, D and E had diameters of 22, 16, 11, 11 and 10 nm, respectively.

The long-lived current blockades did not occur in every nanopore, or at every concentration. When "fluctuating" events occurred, they often began suddenly and occurred at a high frequency for short intervals, only to cease again. We call these events "gating" and they do not appear to have a simple concentration dependence (**Fig. S8**). Two protocols were followed in concentration dependent measurements. In both cases, BSA was added to the *cis* side of the chamber. In the first data set, concentration experiments were performed in 1M KCl, 10mM potassium phosphate, pH 6 at a voltage of +120 mV. Initial concentration of BSA was 10 nM. A 10 minute current trace was performed at each interval. Concentrations were raised in staggered intervals until clogging occurred. In the later data set, experiments were performed at 1M KCl, 10 mM potassium phosphate, pH 7.4. Initial BSA

concentrations were 20 nM. They were raised in 20 nM increments until reaching 180 nM or clogging occurred. The majority of experiments ended when the nanopore "clogged" (**Fig. S9**), making it impossible to continue measurements. We interpret this state as an irreversible absorption of BSA moleculesto the nanopore's inner surface. BSA-induced short-lived current blockades ceased entirely in the clogged state. Experiments were not performed in the reverse order, meaning high concentration to low, due to clogging at high concentrations.

Table S2

Diameter (nm)	Voltage (mV)	Concentration at onset (nM)
9	150	10
10	150	-NA-
10	150	20
10	120	59
12	150	180
12	150	180
12	150	-NA-
12	150	180
14	150	60
14	120	110
14	150	120
14	150	60
14	120	15
14	120	59
15	120	-NA-
15	120	75
15	120	45
16	120	80
16	150	-NA-
16	150	180
16	150	120
17	120	-NA-
20	150	120
20	150	60
20	150	60
22	150	20
22	120	59

Figure S8

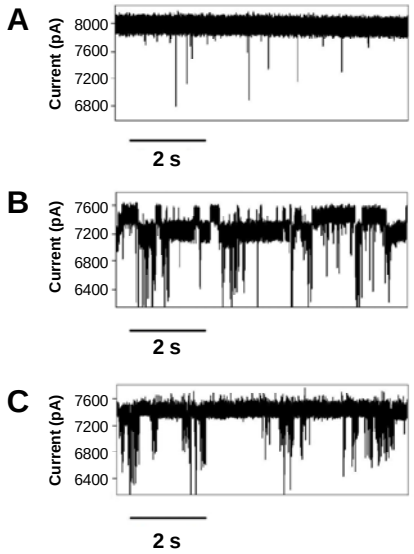

Figure S8. Representative states of pore. (A) BSA-induced current blockades prior to gating state, (B) Long-lived current blockades occurring during the "gating" state, (C) "Clustering" of gating events. Data was taken with a 10 nm pore in 1 M KCl, 10 mM potassium phosphate, pH 7.4. 20 nM BSA was added to the *cis* chamber. The transmembrane potential was +150 mV. The electrical traces were low-pass Bessel filtered at 10 kHz.

Table S2. Summary of the concentrations at which the onset of the long-lived current blockades occurred. In some experiments, nanopores experienced clogging before the long-lived current blockades occurred; these cases were excluded from analysis unless a BSA concentration of 180 nM was reached. "–NA-"signifies the pore clogged (**Fig. S9**).

Figure S9

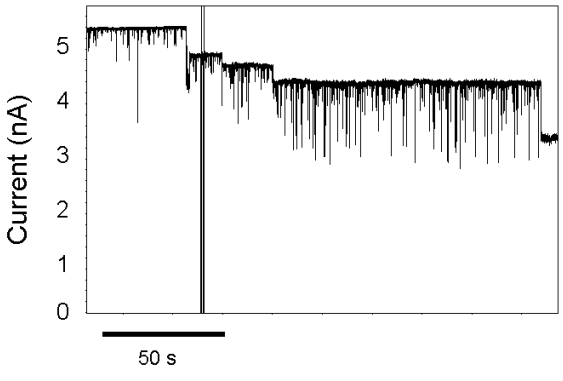

Figure S9. Trace showing the adsorptions of BSA molecules to interior of the pore wall, resulting in a final "clogging" of the pore in which short lived events end. This single-channel electrical trace was recorded with a 10 nm-wide nanopore. 450 nM BSA was added to the *cis* chamber. The buffer solution contained 1M KCl, 10 mM potassium phosphate, pH 7.4. The applied transmembrane potential was +150 mV. The trace was filtered at 2 kHz.

9. Observation of small polypeptides with narrower solid-state nanopores

BSA-induced current blockades were not observed with nanopores smaller than 8 nm in diameter. Our interpretation is that the bulk of the BSA is too large to enter nanopores smaller than this size. To confirm that that this observation is not an artifact of our nanopores, we show events in a 4 nm-wide nanopore due to the 55 residue-long viral nucleocapside polypeptide NCp7 of the HIV-1 virus.[13-16]

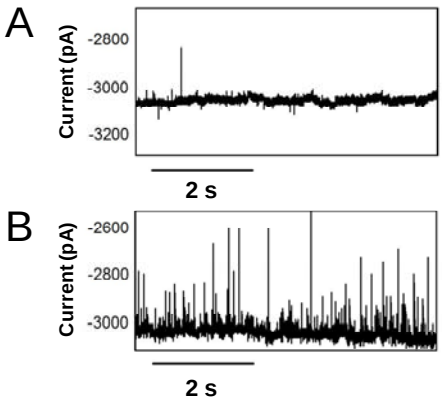

Figure S10. The viral nucleocapside polypeptide NCp7 of the HIV-1 virus produces short-lived current blockades with a small nanopore. (A) Control trace without NCp7, (B) 100 nM NCp7 added to the *cis* chamber. The diameter of the nanopore was 4 nm. The buffer solution was 1M KCl, 10 mM potassium phosphate, pH 7.4. The applied transmembrane potential was -450 mV. When measuring with a 100 kHz filter, the median τ_{off} was 15μs. This places an upper bound on the τ_{off}.

Reference List

1. Kim, M.-J.; Wanunu, M.; Bell, C. D.; Meller, A. Rapid Fabrication of Uniform Size Nanopores and Nanopore Arrays for Parallel DNA Analysis. *Adv. Mater.* **2006,** *18*, 3149-3153.

2. Storm, A. J.; Chen, J. H.; Ling, X. S.; Zandbergen, H. W.; Dekker, C. Fabrication of solid-state nanopores with single-nanometre precision. *Nat. Mater.* **2003,** *2* (8), 537-540.

3. Sackmann, B.; Neher, E. *Single-Channel Recording;* Second Edition ed.; Kluwer Academic/Plenum Publishers: New York, 1995.

4. Movileanu, L.; Howorka, S.; Braha, O.; Bayley, H. Detecting protein analytes that modulate transmembrane movement of a polymer chain within a single protein pore. *Nat. Biotechnol.* **2000,** *18* (10), 1091-1095.

5. Wanunu, M.; Meller, A. Chemically modified solid-state nanopores. *Nano. Lett.* **2007,** *7* (6), 1580-1585.

6. Hoogerheide, D. P.; Garaj, S.; Golovchenko, J. A. Probing surface charge fluctuations with solid-state nanopores. *Phys. Rev. Lett.* **2009,** *102* (25), 256804.

7. Wanunu, M.; Meller, A. Single-molecule analysis of nucleic acids and DNA-protein interactions. In *Single-molecule techniques: a laboratory manual*, Selvin, P. R., Ha, T., Eds.; Cold Spring Harbor Laboratory Press: New York, 2008; pp 395-420.

8. Bohme, U.; Scheler, U. Effective charge of bovine serum albumine determined by electrophoresis NMR. *Chem. Phys. Lett.* **2007,** *435*, 342-345.

9. Movileanu, L.; Cheley, S.; Bayley, H. Partitioning of individual flexible polymers into a nanoscopic protein pore. *Biophys. J.* **2003,** *85* (2), 897-910.

10. Bevington, P. R.; Robinson, D. K. *Data Reduction and Error Analysis for the Physical Sciences;* 3rd Edition ed.; McGraw Hill: 2003.

11. Gregg, E. C.; Steidley, K. D. Electrical counting and sizing of mammalian cells in suspension. *Biophys. J.* **1965,** *5* (4), 393-405.

12. DeBlois, R. W.; Bean, C. P. Counting and sizing of submicron particles by resistive pulse technique. *Rev. Sci. Instrum.* **1970,** *41* (7), 909-917.

13. De Guzman, R. N.; Wu, Z. R.; Stalling, C. C.; Pappalardo, L.; Borer, P. N.; Summers, M. F. Structure of the HIV-1 nucleocapsid protein bound to the SL3 psi-RNA recognition element. *Science* **1998,** *279* (5349), 384-388.

14. Paoletti, A. C.; Shubsda, M. F.; Hudson, B. S.; Borer, P. N. Affinities of the nucleocapsid protein for variants of SL3 RNA in HIV-1. *Biochemistry* **2002,** *41* (51), 15423-15428.

15. Shubsda, M. F.; Paoletti, A. C.; Hudson, B. S.; Borer, P. N. Affinities of packaging domain loops in HIV-1 RNA for the nucleocapsid protein. *Biochemistry* **2002,** *41* (16), 5276-5282.

16. Yuan, Y.; Kerwood, D. J.; Paoletti, A. C.; Shubsda, M. F.; Borer, P. N. Stem of SL1 RNA in HIV-1: structure and nucleocapsid protein binding for a 1 x 3 internal loop. *Biochemistry* **2003,** *42* (18), 5259-5269.